

# RANDOM FIELD REPRESENTATION OF HORIZONTAL DENSITY DISTRIBUTION IN PARTIALLY ORIENTED STRANDBOARD MAT

*Congjin Lu*

Former Graduate Research Assistant  
SydneyPLUS International Library System  
Richmond, BC  
Canada V6V 2J7

and

*Frank Lam*<sup>†</sup>

Associate Professor  
Department of Wood Science, Faculty of Forestry  
University of British Columbia  
Vancouver, BC  
Canada V6T 1Z4

(Received July 2000)

## ABSTRACT

A random field representation of the horizontal density distribution in partially oriented strandboard mats was investigated. The orientation of strands can be characterized by both the von Mises distribution and the uniform distribution within a range of angles. Theoretical models of the correlation coefficients of any two points simultaneously covered by one strand, characteristic area of the correlation, and the degree of orientation were developed. Results indicate that the concentration factor  $k = 700$  is sufficiently large to represent a perfectly aligned strand arrangement in oriented strandboards based on the von Mises distribution. The correlation coefficients of two points in a mat have a lower bound (random case) and an upper bound (perfectly aligned) in both von Mises and uniform distributions. Based on the concept of characteristic area, where the minimum characteristic area is the area of the strand and the maximum characteristic area is approximate to the square of strand length, the degree of orientation in a panel can be represented as a function of characteristic area. This value is found to be very close to the percent alignment definition.

*Keywords:* Random field, mathematical model, horizontal density distribution, auto-correlation function, partially oriented strandboard, von Mises distribution, uniform distribution, characteristic area, degree of orientation.

## INTRODUCTION

Oriented strandboards (OSB) are made by processing relatively low value and underutilized wood materials into strands, which are approximately 100 mm in length, 15–20 mm in width, and roughly 0.6–0.8 mm in thickness. After the strands are dried, adhesives and wax are applied, and the strands are typically formed into a three-layer mat. The top and bottom (face) layers are partially oriented along the long axis of the panel to provide

added bending strength and stiffness in the direction of orientation, while strands in the middle (core) layer of the mat are randomly oriented or partially oriented in the perpendicular direction of the face layers. The mat is bonded together under heat and pressure to produce panels of various dimensions and thicknesses. OSB panels are very versatile as their mechanical and physical properties can be controlled by adjustment of production parameters to meet end users' demands for such characteristics as size, density, and strength. The various production parameters that influence OSB performance include species, strand

---

<sup>†</sup> Member of SWST

geometry, strand lay up/orientation process (strandboard structure), adhesive type and distribution mechanism, and pressing process. Many researchers have shown great interest in strandboard structures and properties (Dai and Steiner 1994; Land and Wolcott 1996; Suchsland and Xu 1989; Triche and Hunt 1993; Xu and Steiner 1995; Lu et al. 1998). In particular, Dai and Steiner (1994) studies the spatial correlation of strand coverage by making use of the theories in random fibrous network (Dodson 1971) to define the horizontal density distribution in panels with completely random strand orientation and position. The statistics of the horizontal density distribution in OSB are of particular interest in the assessment of product quality and performance. While most of the research has focused on completely random orientation of strands and its influences on physical and mechanical strength properties of the panels, the strand orientation in both face layers of OSB is in reality, partially random. There has been no theoretical consideration of the relationship between partially random orientation of strandboards with physical properties such as the variation of board density in the horizontal direction in the OSB products. Since two orientation angles  $\theta$  and  $\theta + n\pi$  ( $n = 1, 2, 3, \dots$ ) cannot be distinguished for a rectangular strand placed in a mat, the range of angles from  $-\pi/2$  to  $+\pi/2$  radian can completely describe all possible choices for strand orientation. The random distribution of strand orientation within a mat is an excellent example of axial data, which can be best described by the von Mises distribution (Mardia 1972). Harris and Johnson (1982) pointed out that the concentration parameter of the von Mises distribution ( $k$ ) can be used to characterize the distribution of strand orientations in strandboards. Shaler (1991) compared two measures of strand alignment based on the von Mises distribution of strand alignment and the classical definition of percent alignment given by Geimer (1976), which in fact is a linear transformation of the first moment (arithmetic mean) of the absolute value of angles in the range of  $\pm\pi/2$  radian. Computer simulations

yielded good agreement with theoretical calculations (Shaler 1991). Lau (1981) linked the standard deviation of normal distribution with the range of orientation angles by a factor of  $\sqrt{\pi/2}$ .

This paper presents a theoretical model of the horizontal density distribution of partially oriented strandboard mat. The objectives of this study are:

- 1) to develop a random field representation of horizontal density distribution for partially oriented strandboards following the von Mises distribution and the uniform distribution,
- 2) to introduce the concept of characteristic area as a measure of within member correlation of horizontal density distribution, and
- 3) to characterize the degree of orientation as compared with the traditional definition of percent alignment (Geimer 1976).

#### THEORETICAL MODEL

##### *Probability density function for strand orientation*

Due to the forming process of OSB, the orientation of the principal direction of each strand is partially random. Mardia (1972) provided a comprehensive description of the statistics of directional data. One of the most important properties of such a random variable  $\theta$  (in radian) is that its probability density function  $f(\theta)$  has a circular form:

$$f(\theta \pm n\pi) = f(\theta) \quad \left( -\frac{\pi}{2} \leq \theta \leq \frac{\pi}{2} \right) \\ (n = 1, 2, 3, \dots) \quad (1)$$

since a strand oriented at  $\theta$  to the  $x$  direction is the same as a strand oriented at  $\theta \pm n\pi$ . A function for characterizing directional axial data is the von Mises probability density function (PDF) whose axial functional form is derived from Mardia (1972), and Harris and Johnson (1982):

$f(\theta, \theta_1, k)$

$$= \begin{cases} \frac{1}{2\theta_1 I_0(k)} e^{k \cos[2(\theta-\theta_0)]} & \left(-\theta_1 \leq \theta \leq \theta_1, \text{ and } 0 < \theta_1 \leq \frac{\pi}{2}\right) \\ 0 & \text{otherwise} \end{cases} \quad (2)$$

where  $k$  is the concentration parameter to specify the shape of the distribution,  $\theta_0$  is the mean value of the orientation angles,  $\theta_1$  equals to  $\pi/2$  when  $k > 0$ , which means that the range of strand orientation angles in the von Mises distribution must be between  $-\pi/2$  and  $\pi/2$ , and

$$I_0(k) = \sum_{m=0}^{\infty} \frac{1}{(m!)^2} \left(\frac{1}{2}k\right)^{2m}$$

is the modified Bessel function of the first kind, order zero (Mardia 1972). Another property of this PDF is that the integration of the PDF over the range of  $-\pi/2 \leq \theta \leq \pi/2$  equals to one, i.e.,

$$\int_{-\theta_1}^{\theta_1} f(\theta, \theta_1, k) d\theta = \frac{1}{2\theta_1 I_0(k)} \int_{-\theta_1}^{\theta_1} e^{k \cos[2(\theta-\theta_0)]} d\theta = 1 \quad (3)$$

By re-arranging Eq. 3,  $2\theta_1 I_0(k)$  can be expressed as:

$$2\theta_1 I_0(k) = \int_{-\theta_1}^{\theta_1} e^{k \cos[2(\varphi-\theta_0)]} d\varphi \quad (4)$$

A PDF without the Bessel function can be obtained by combining Eq. (4) into Eq. (2) as:

$$f(\theta, \theta_1, k) = \frac{e^{k \cos[2(\theta-\theta_0)]}}{\int_{-\theta_1}^{\theta_1} e^{k \cos[2(\varphi-\theta_0)]} d\varphi} \quad (5)$$

When  $k \rightarrow 0$ ,  $f(\theta, \theta_1, 0) = 1/2\theta_1$ , which represents a uniform distribution of orientation angles. When  $k \rightarrow \infty$ , the distribution reduces to a point distribution, which can be described

by the Dirac delta function (the perfectly aligned case).

*Correlation coefficient for two points in a rectangle*

Consider the distribution of two-dimensional strands with length  $\lambda$  and width  $\omega$  ( $\omega \leq \lambda$ ); it is assumed that the long axes of these strands are oriented at an angle of  $\theta + d\theta$  from a given reference direction, usually  $x$  direction. The random locations of the strand centroids are assumed to follow a Poisson distribution (Dai and Steiner 1994) of overlap intensity  $d\mu(\theta)$  per unit area. Therefore, the superposition of such processes (Dodson 1971), for  $-\pi/2 < \theta \leq \pi/2$ , produces a distribution of overlaps with intensity  $\mu$  per unit area for the total number of strand centers as:

$$d\mu(\theta, \theta_1, k) = \mu f(\theta, \theta_1, k) d\theta = \frac{\mu e^{k \cos[2(\theta-\theta_0)]}}{\int_{-\theta_1}^{\theta_1} e^{k \cos[2(\varphi-\theta_0)]} d\varphi} d\theta \quad (6)$$

Correlation coefficient,  $\alpha$ , between the number of strand overlaps at two points,  $p$  and  $q$  separated by a distance of  $r$  is given as (Dodson 1971),

$$\alpha(\lambda, \omega, \theta_1, k, r) = \frac{\text{var}(N_{pq})}{\text{var}(N_p)} \quad (7)$$

where  $N_{pq}$  is the number of strands that cover both  $p$  and  $q$ , and  $N_p$  is the total number of strands that cover only  $p$ . It is obvious that both  $N_{pq}$  and  $N_p$  are Poisson distributed with the variances equal to

$$\text{var}(N_p) = \int_{-\theta_1}^{\theta_1} \lambda \omega d\mu(\theta) = \lambda \omega \mu \quad (8)$$

$$\text{var}(N_{pq}) = \int_{-\theta_1}^{\theta_1} (\omega - r \sin|\theta|) \times (\lambda - r \cos \theta) d\mu(\theta) \quad (9)$$

where  $(\omega - r \sin|\theta|)(\lambda - r \cos \theta)$  is the total area containing the centers of strands that cover both  $p$  and  $q$ . Applying  $d\mu(\theta)$  from Eq. (6) into Eq. (9) and combining Eqs. (7) to (9), it can be shown that the correlation coefficient,  $\alpha$ , is:

$$\begin{aligned} \alpha(\lambda, \omega, \theta_1, k, r) &= \frac{\text{var}(N_{pq})}{\text{var}(N_p)} \\ &= \frac{\int_{-\theta_1}^{\theta_1} \left(1 - \frac{r}{\omega} \sin|\theta|\right) \left(1 - \frac{r}{\lambda} \cos \theta\right) e^{k \cos[2(\theta-\theta_0)]} d\theta}{\int_{-\theta_1}^{\theta_1} e^{k \cos[2(\varphi-\theta_0)]} d\varphi} \end{aligned} \tag{10}$$

where  $r$  equals to the distance separated by two points  $p$  and  $q$ .

For all possible values of  $\theta$  within the rectangular domain  $\lambda \times \omega$ , using the symmetry properties of  $(\omega - r \sin|\theta|)(\lambda - r \cos \theta)$ , three ranges of angles are necessary to be taken into consideration where  $\Omega$  represents the integration intervals for  $\theta$  at  $\theta_1 = \pi/2$ .

- 1)  $0 < r \leq \omega$ , corresponding to  $\Omega = \{0 < \theta \leq 1/2\pi\}$ ;

- 2)  $\omega < r \leq \lambda$ , corresponding to  $\Omega = \{0 < \theta \leq \arcsin(\omega/r)\}$ ;
- 3)  $\lambda < r \leq \sqrt{\lambda^2 + \omega^2}$ , corresponding to  $\Omega = \{\arccos(\lambda/r) < \theta \leq \arcsin(\omega/r)\}$ .

The correlation coefficient  $\alpha(\lambda, \omega, \theta_1, k, r)$  can be evaluated at arbitrary  $r$  and  $k$  ( $k \neq 0$ ). Of special interest are the limiting cases of  $k = 0$  and  $k = \infty$ , which will be discussed in more detail as follows.

In cases where  $k = 0$  and  $\theta_1 \leq \pi/2$ , the von Mises distribution becomes the uniform distribution with PDF of the following form:

$$f(\theta, \theta_1, 0) = \frac{1}{2\theta_1} \left( -\theta_1 < \theta \leq \theta_1, \text{ and } 0 < \theta_1 \leq \frac{\pi}{2} \right) \tag{11}$$

Here  $\pm\theta_1$  are the upper and lower bounds for orientation angle  $\theta$ . It can take arbitrary values from 0 to  $\pi/2$ . If  $\theta_1$  approaches zero, all strands are oriented parallel to each other; if  $\theta_1$  equals  $\pi/2$ , it is completely randomized orientation. In the general case of partially random orientation,  $0 < \theta_1 \leq \pi/2$ , the exact form of the correlation coefficient is given for the three ranges of  $\theta_1$  shown in Fig. 1 and detailed in Appendix A as follows:

---

Case 1:  $\arcsin(\omega/\lambda) < \theta_1 \leq \pi/2$

$$\begin{aligned} \alpha(\lambda, \omega, \theta_1, 0, r) &= \begin{cases} \left[ 1 - \frac{1}{\theta_1} \left[ \frac{r}{\lambda} \sin \theta_1 - \frac{r}{\omega} (\cos \theta_1 - 1) - \frac{r^2}{2\lambda\omega} \sin^2 \theta_1 \right] \right] & \left( 0 < r \leq \frac{\omega}{\sin \theta_1} \right) \\ \left[ \frac{1}{\theta_1} \left[ \arcsin\left(\frac{\omega}{r}\right) - \frac{\omega}{2\lambda} - \frac{r}{\omega} + \frac{\sqrt{r^2 - \omega^2}}{\omega} \right] \right] & \left( \frac{\omega}{\sin \theta_1} < r \leq \lambda \right) \\ \left[ \frac{1}{\theta_1} \left[ \arcsin\left(\frac{\omega}{r}\right) - \arccos\left(\frac{\lambda}{r}\right) - \frac{\lambda^2 + \omega^2 + r^2}{2\lambda\omega} + \frac{\sqrt{r^2 - \omega^2}}{\omega} + \frac{\sqrt{r^2 - \lambda^2}}{\lambda} \right] \right] & \left( \lambda < r \leq \sqrt{\lambda^2 + \omega^2} \right) \end{cases} \end{aligned} \tag{12}$$

Case 2:  $\arcsin(\omega/\sqrt{\lambda^2 + \omega^2}) < \theta_1 \leq \arcsin(\omega/\lambda)$

$\alpha(\lambda, \omega, \theta_1, 0, r)$

$$= \begin{cases} 1 - \frac{1}{\theta_1} \left[ \frac{r}{\lambda} \sin \theta_1 - \frac{r}{\omega} (\cos \theta_1 - 1) - \frac{r^2}{2\lambda\omega} \sin^2 \theta_1 \right] & (0 < r \leq \lambda) \\ 1 - \frac{1}{\theta_1} \left[ \arccos\left(\frac{\lambda}{r}\right) + \frac{r}{\lambda} \sin \theta_1 - \frac{r}{\omega} \cos \theta_1 - \frac{r^2}{2\lambda\omega} \sin^2 \theta_1 + \frac{\lambda^2 + r^2}{2\lambda\omega} - \frac{\sqrt{r^2 - \lambda^2}}{\lambda} \right] & \left( \lambda < r \leq \frac{\omega}{\sin \theta_1} \right) \\ \frac{1}{\theta_1} \left[ \arcsin\left(\frac{\omega}{r}\right) - \arccos\left(\frac{\lambda}{r}\right) - \frac{\lambda^2 + \omega^2 + r^2}{2\lambda\omega} + \frac{\sqrt{r^2 - \omega^2}}{\omega} + \frac{\sqrt{r^2 - \lambda^2}}{\lambda} \right] & \left( \frac{\omega}{\sin \theta_1} < r \leq \sqrt{\lambda^2 + \omega^2} \right) \end{cases} \quad (13)$$

Case 3:  $0 < \theta_1 \leq \arcsin(\omega/\sqrt{\lambda^2 + \omega^2})$

$\alpha(\lambda, \omega, \theta_1, 0, r)$

$$= \begin{cases} 1 - \frac{1}{\theta_1} \left[ \frac{r}{\lambda} \sin \theta_1 - \frac{r}{\omega} (\cos \theta_1 - 1) - \frac{r^2}{2\lambda\omega} \sin^2 \theta_1 \right] & (0 < r \leq \lambda) \\ 1 - \frac{1}{\theta_1} \left[ \arccos\left(\frac{\lambda}{r}\right) + \frac{r}{\lambda} \sin \theta_1 - \frac{r}{\omega} \cos \theta_1 - \frac{r^2}{2\lambda\omega} \sin^2 \theta_1 + \frac{\lambda^2 + r^2}{2\lambda\omega} - \frac{\sqrt{r^2 - \lambda^2}}{\lambda} \right] & \left( \lambda < r \leq \frac{\lambda}{\cos \theta_1} \right) \end{cases} \quad (14)$$

It is noted that when  $\theta_1 = \pi/2$ , Eq. (12) represents the completely random case in the following form, which agrees with the finding of Dodson (1971).

$$\alpha\left(\lambda, \omega, \frac{\pi}{2}, 0, r\right) = \begin{cases} 1 - \frac{2}{\pi} \left[ \frac{r}{\lambda} + \frac{r}{\omega} - \frac{r^2}{2\lambda\omega} \right] & (0 < r \leq \omega) \\ \frac{2}{\pi} \left[ \arcsin\left(\frac{\omega}{r}\right) - \frac{\omega}{2\lambda} - \frac{r}{\omega} + \frac{\sqrt{r^2 - \omega^2}}{\omega} \right] & (\omega < r \leq \lambda) \\ \frac{2}{\pi} \left[ \arcsin\left(\frac{\omega}{r}\right) - \arccos\left(\frac{\lambda}{r}\right) - \frac{\lambda^2 + \omega^2 + r^2}{2\lambda\omega} + \frac{\sqrt{r^2 - \omega^2}}{\omega} + \frac{\sqrt{r^2 - \lambda^2}}{\lambda} \right] & (\lambda < r \leq \sqrt{\lambda^2 + \omega^2}) \end{cases} \quad (15)$$

If all strands are perfectly aligned ( $\theta_1 = 0$ ), the correlation coefficient is a function of strand length ( $\lambda$ ) and the distance ( $r$ ) between two arbitrarily chosen points on a line. When

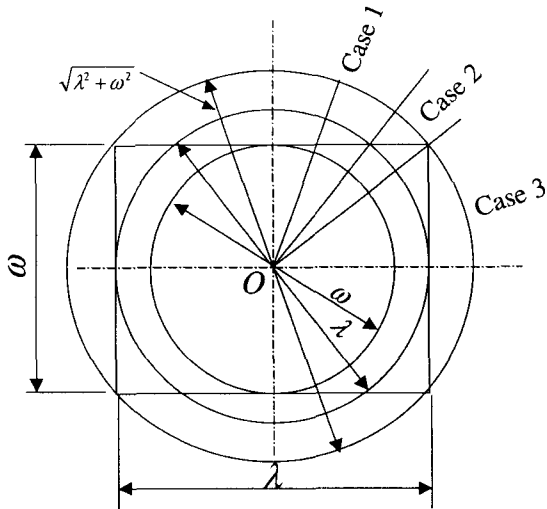


FIG. 1. Schematic diagram of three cases for a strand with length  $\lambda$  and width  $\omega$  during integration.

$r = 0$ , the two points are common and the correlation coefficient equals unity. When the distance  $r$  between two points is greater than  $\lambda$ , the correlation coefficient is zero. It can be summarized as:

$$\alpha(\lambda, \omega, 0, 0, r) = \begin{cases} 1 - \frac{r}{\lambda} & (0 \leq r \leq \lambda) \\ 0 & (r > \lambda) \end{cases} \quad (16)$$

*Characteristic area—a measure of correlation*

In random field theory, the “characteristic area” is an important statistical parameter, which defines a measure of correlation. It is a proportional constant which equals the integration of the correlation function ( $\alpha$ ) (Vanmarcke 1983):

$$A(\lambda, \omega, \theta_1, k) = \int_{-\infty}^{+\infty} \int_{-\infty}^{+\infty} \alpha(x, y) dx dy = \int_0^{r_{max}} 2\pi r \cdot \alpha(\lambda, \omega, \theta_1, k, r) dr \quad (17)$$

In the case of perfectly oriented situation (Eq. 16), the characteristic area is given by:

$$A(\lambda, \omega, 0, 0) = \int_0^\lambda 2\pi r \cdot \left(1 - \frac{r}{\lambda}\right) dr = \frac{1}{3} \pi \lambda^2 \cong \lambda^2 \quad (18)$$

For completely randomized strand orientation (Eq. 15), the characteristic area can be evaluated by following the procedures given in Appendix B as:

$$A\left(\lambda, \omega, \frac{\pi}{2}, 0\right) = \int_0^{\sqrt{\lambda^2 + \omega^2}} 2\pi r \cdot \alpha\left(\lambda, \omega, \frac{\pi}{2}, 0, r\right) dr = \lambda \omega \quad (19)$$

which is equal to the area of strand.

*Degree of orientation*

A conventional definition of percent alignment (Eq. 20) was introduced by Geimer (1976), which measures the mean angle deviation from  $45^\circ$  to the geometric axes of the sample.

$$Align\% = \frac{45 - \theta}{45} \times 100 \quad (20)$$

where

$$\theta = \frac{1}{n} \sum_{i=1}^n |\theta_i|$$

$\theta_i = i^{th}$  measured angle, and

$n =$  number of measurements.

Angles are measured over the range of  $-90^\circ$  to  $+90^\circ$  with the  $0^\circ$  being the assumed mean angle. This definition can be used to define strand alignment in experimental mat where strand angles can be established. For a real board, it is more difficult to peel off the strands layer by layer to measure the angles. Alternately, nondestructive testing method can be used to extract the horizontal density dis-

tribution of a sample board, and random field theory can be used to evaluate the degree of orientation as described below.

As discussed earlier, the strand alignment can be random ( $k = 0$  in the von Mises distribution,  $\theta_1 = \pi/2$  in the uniform distribution) and perfectly aligned ( $k = \infty$  in the von Mises distribution,  $\theta_1 = 0$  in the uniform distribution). It is reasonable to consider the random orientation case as zero degree of orientation, and perfectly aligned orientation case (all strands parallel to long axis of the panel) as 100% degree of orientation. From Figs. 2 and 3, it is easily seen that all the correlation co-

efficients lie within these two curves, random and oriented. Therefore, the area between any particular curve and the curve for the random case is indirectly related to the degree of strand orientation. This provided a base to define the degree of orientation of strand, *Orient* (%). The integration of correlation function ( $\alpha$ ) is actually the characteristic area  $A$  for any given range of angles in the uniform distribution and any value of  $k$  in the von Mises distribution.

By applying the results from Eqs. (18) and (19), the degree of orientation (*Orient*) can be obtained:

$$\left. \begin{aligned}
 \text{Orient}(k) &= \sqrt{\frac{A\left(\lambda, \omega, \frac{\pi}{2}, k\right) - A\left(\lambda, \omega, \frac{\pi}{2}, 0\right)}{A\left(\lambda, \omega, \frac{\pi}{2}, \infty\right) - A\left(\lambda, \omega, \frac{\pi}{2}, 0\right)}} \times 100 = \sqrt{\frac{A\left(\lambda, \omega, \frac{\pi}{2}, k\right) - \lambda\omega}{\frac{1}{3}\pi\lambda^2 - \lambda\omega}} \times 100 \\
 \text{Orient}(\theta_1) &= \sqrt{\frac{A\left(\lambda, \omega, \theta, 0\right) - A\left(\lambda, \omega, \frac{\pi}{2}, 0\right)}{A\left(\lambda, \omega, 0, 0\right) - A\left(\lambda, \omega, \frac{\pi}{2}, 0\right)}} \times 100 = \sqrt{\frac{A\left(\lambda, \omega, \theta, 0\right) - \lambda\omega}{\frac{1}{3}\pi\lambda^2 - \lambda\omega}} \times 100
 \end{aligned} \right\} \tag{21}$$

Here, the square root is applied to make it compatible to the percent alignment because the percent alignment is a linear transformation of the mean angles.

*Evaluation of density image autocorrelation*

A two-dimensional autocorrelation function (ACF) and the degree of orientation for a commercial panel can be readily evaluated, provided that the density measurements of the panel in the horizontal plane  $D(x, y)$  can be obtained through some nondestructive testing methods. To determine the ACF of a digitized image, the autocovariance is calculated first as

a function of various offsets and is given by Agterberg (1974) as:

$$C(r, s) = \frac{1}{(N_x - r)(N_y - s)} \sum_{x=0}^{N_x-r-1} \sum_{y=0}^{N_y-s-1} \times (D_{x,y} - \bar{D})(D_{x+r,y+s} - \bar{D}) \tag{22}$$

where  $N_x$  and  $N_y$  are the number of pixels of the image in the  $x$ - and  $y$ -directions,  $r$  and  $s$  are the offsets in the  $x$ - and  $y$ -directions,  $x$  and  $y$  are the pixel coordinates in the image, and  $\bar{D}$  is the average value of density in the image.

It is obvious that  $C(0, 0)$ , which corresponds to zero offset, is the variance of density

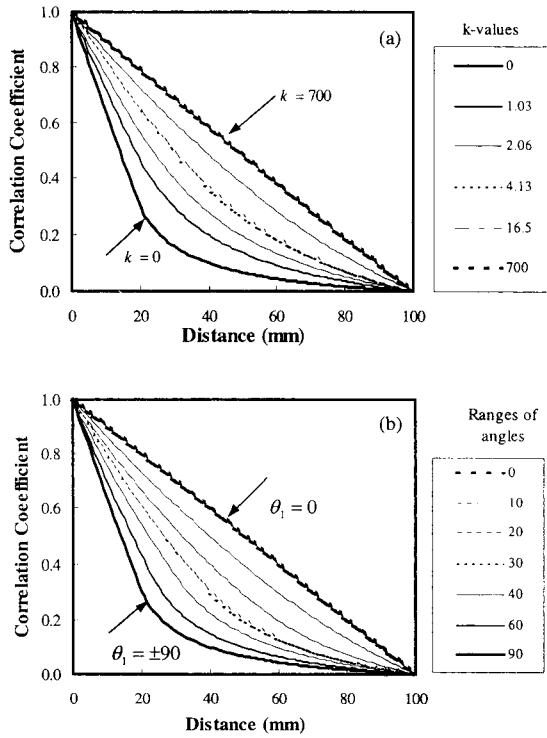


FIG. 2. Correlation coefficients: (a) for different values of concentration parameter  $k$  in von Mises distribution, and (b) for different ranges of angles  $\theta_1$  (angles represent  $\pm$ ) in uniform distribution (strand length 100 mm and width 20 mm).

in the image. Therefore, the autocorrelation,  $Auto(r, s)$ , is obtained by dividing  $C(r, s)$  by the  $C(0, 0)$  (Agterberg 1974; Pfeiderer et al. 1993) as:

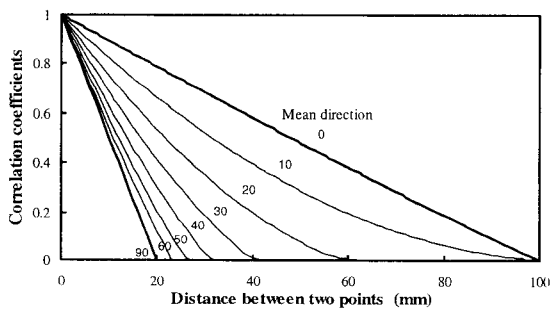


FIG. 3. Correlation coefficient between two points in the mat with various mean direction ( $\theta_0$ ) in von Mises distribution (strand length 100 mm and width 20 mm,  $k = 700$ ).

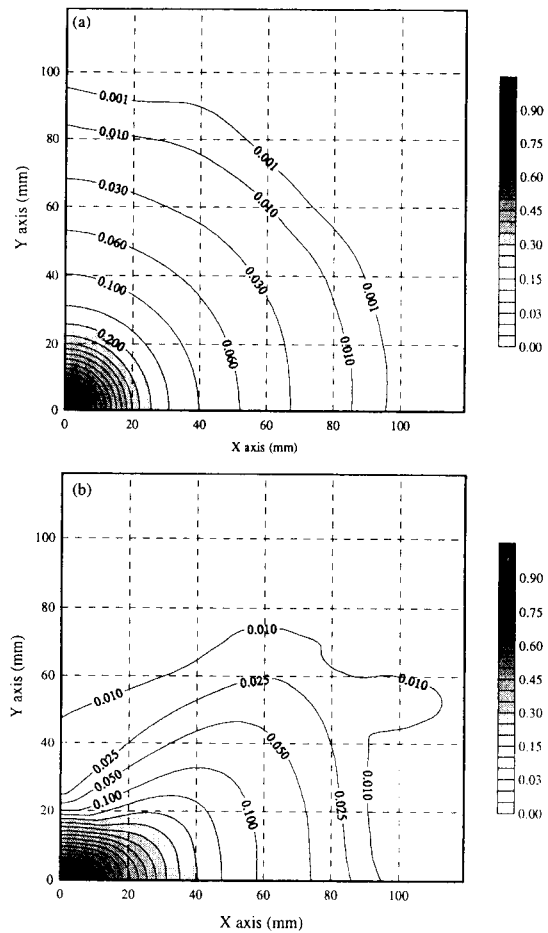


FIG. 4. Correlation coefficient between two points in a mat: (a) in completely randomized distribution of strand location and orientation, (b) with partial orientation of strands (range of angles:  $-45$  to  $+45$  degrees), and (c) in perfectly aligned strand orientation ( $0^\circ$ ) and random location (strand length 100 mm and width 20 mm).

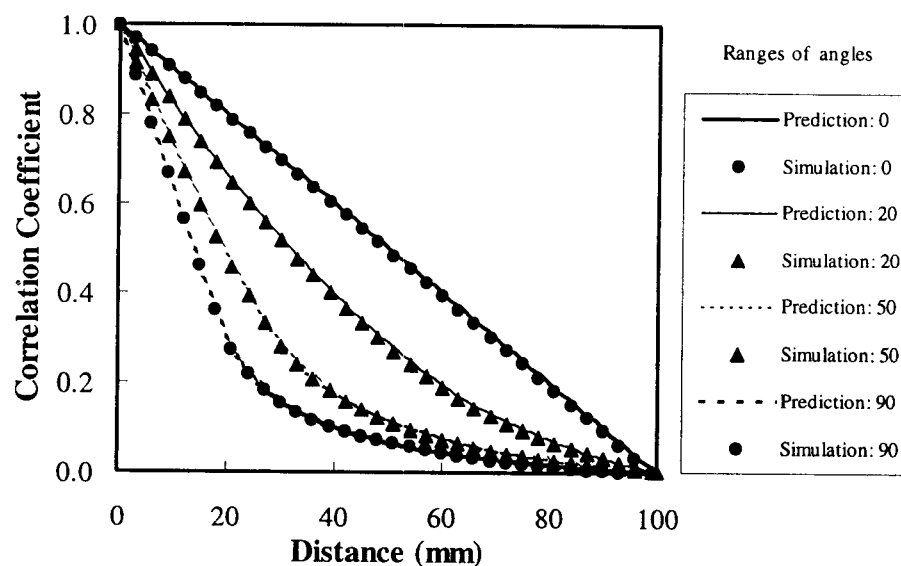


FIG. 5. Comparison of correlation coefficients between model prediction (lines) and computer simulation (markers) (strand length 100 mm and width 20 mm).

$$Auto(r, s) = \frac{C(r, s)}{C(0, 0)} \quad (23)$$

For zero offset,  $Auto(0, 0) = 1$ , and with increasing offset,  $Auto(r, s)$  gradually decreases as the pixels become more and more independent or statistically uncorrelated. However, this decrease is anisotropic if strands of the panel are aligned (or partially oriented) along a preferred direction (Fig. 4b and 4c). Therefore, by visualizing the 2D distribution of ACF values, the degree of orientation can be calculated by Eq. (21). In this paper, all the digitized images are obtained by Monte Carlo Simulations (Lu et al. 1998).

#### RESULTS AND DISCUSSION

##### *Autocorrelation coefficient of density*

It can be noted that the autocorrelation coefficients of density for any two points in a mat domain are bounded with the random case as the lower bound and perfectly aligned orientation as the upper bound. Increasing the concentration parameter  $k$  from 0 to infinity (in the von Mises distribution) or decreasing the range of orientation angle  $\theta_1$  from  $\pi/2$  to 0 (in the uniform distribution) moves the au-

tocorrelation coefficient of density curve from its lower bound towards its upper bound (Fig. 2a and 2b).

Strand length and width are the two other factors influencing the shape of the autocorrelation coefficient of density curves since any two points covered by one larger strand may not be covered by a smaller strand. If strand length is much greater than the width ( $\lambda \gg \omega$ ), the density autocorrelation coefficient is simplified to only one case (Eq. 12). When the mean angle ( $\theta_0$ ) changes from 0 to  $\pi/2$  at  $k = \infty$  ( $k = 700$  in our case), the zero autocorrelation coefficient also changes from  $r = \lambda$  to  $r = \omega$  (Fig. 3). Figures 4a to 4c present the contour autocorrelation coefficients of density for three simulated mats. It is obvious that the density autocorrelation coefficient is one when  $x$  and/or  $y$  coordinates (the distance between any two points) are zeros, and zero when  $x$  and/or  $y$  are very large. For the random mat (Fig. 4a), the autocorrelation coefficients form many concentric cycles around the origin. Figure 4b represents the autocorrelation of a partially oriented strandboard mat (range of angles from  $-45$  to  $+45$  degrees). For the perfectly aligned mat (Fig. 4c), the autocorrela-

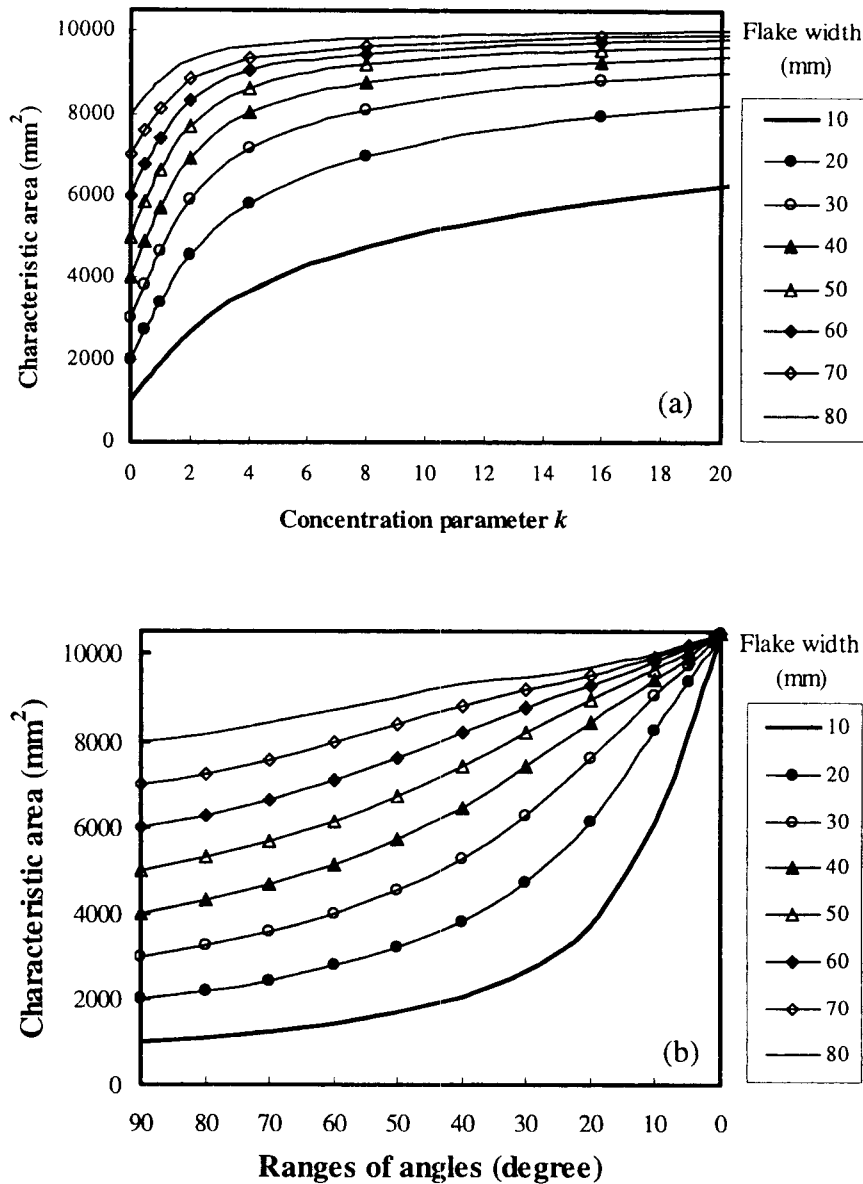


FIG. 6. Characteristic area in relation to (a) the concentration parameter  $k$  in von Mises distribution of strands, and (b) the ranges of angles (angles represent  $\pm$ ) in uniform distribution of strands (strand length 100 mm).

tion coefficient of density is a linear function of the distance between two points along either the strand length direction or the strand width direction. This agrees well with the findings in Fig. 3.

A comparison of the autocorrelation coefficients between model prediction and com-

puter simulation is presented in Fig. 5. The simulation results agree well with the theoretically predicted values. There is a slight deviation between the predicted and simulated values when the size of simulated mat is small because an infinite domain is assumed in the mathematical model.

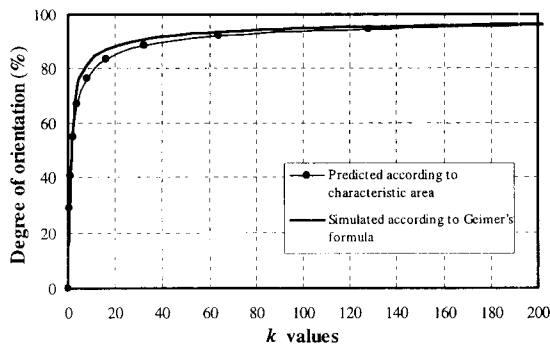


FIG. 7. Degree of orientation of strands with respect to concentration parameter  $k$  in von Mises distribution (strand length 100 mm and width 20 mm).

#### Characteristic area

As another measure of correlation, Fig. 6a and 6b show that the characteristic area increases when the strands become more oriented. It can also be noted that the maximum characteristic area is approximately equal to the square of the strand length in perfectly oriented strandboard mat because it is independent of strand width.

#### Degree of orientation

The degree of orientation of strands was compared with the percent alignment calculated by Geimer's formula for the mean angle at zero degree in the von Mises distribution (Fig. 7) and in the uniform distribution (Fig. 8). The degree of orientation started at 0 for random orientation case and ended at 100% for the perfectly aligned arrangement in both distributions. The predicted and simulated values from characteristic areas agree well with the percent alignment values. This suggests that the degree of orientation concept can also be used to estimate the strand arrangement of commercial panels if the horizontal density distribution of the panel can be evaluated through nondestructive testing.

#### CONCLUSIONS

The degree of orientation of strands in structural wood-based composites, such as OSB, is an important processing parameter because

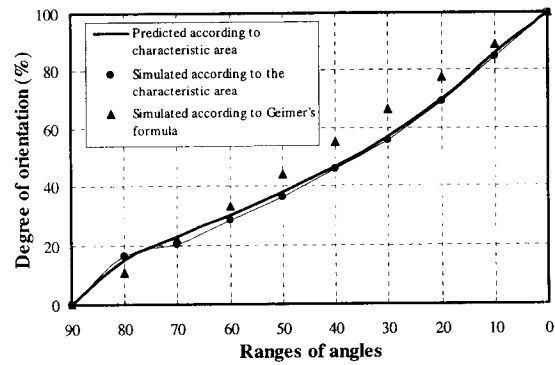


FIG. 8. Degree of orientation of strands with respect to the ranges of angles (angles represent  $\pm$ ) in uniform distribution (strand length 100 mm and width 20 mm).

it determines the degree of directional strength and stiffness of the panel. A random field theory representation of the variation of horizontal density in partially oriented strandboard mats was presented in this study.

The orientation of strands in a mat was characterized by both the von Mises distribution and the uniform distribution within a range of angles. Theoretical models for the correlation coefficients, characteristic area, and the degree of orientation were discussed.

Theoretical analysis indicated that  $k = 700$  is sufficiently large to represent the perfectly aligned orientation of strands in von Mises distribution. The correlation coefficients have a lower bound (random case) and an upper bound (perfectly aligned) in both distributions. Strand geometry and mean orientation angles have great influences on the correlation coefficient.

The characteristic area, another measure of correlation, has the minimum and maximum values, which are expressed as the area of a strand and the approximate square of strand length, respectively. The degree of orientation discussed in this study is an alternate way to estimate the strand alignment of OSB products. However, the degree of orientation obtained by this approach is the overall average in the thickness direction under an assumption of uniform strand size.

ACKNOWLEDGMENTS

The funding provided by NSERC, Forestry Canada, Forintek Canada Corp., McMillan Bloedel Co. (CRD0164104) and Wood Design Fellowship from Weyerhaeuser for this study is gratefully acknowledged.

REFERENCES

AGTERBERG, F. P. 1974. Geomathematics: Athemathical background and geo-science applications. Elsevier Scientific Publishing Co. Amsterdam, Netherlands. 596pp.

DAI, C., AND P. R. STEINER. 1994. Spatial structure of wood composites in relation to processing and performance characteristics. Part 3. Modeling the formation of multi-layered random flake mats. Wood Sci. Technol. 28:229-239.

DODSON, C. T. J. 1971. Spatial variability and the theory of sampling in random fibrous networks. J. Roy. Stat. Soc., Series B, 33(1):82-94.

GEIMER, R. L. 1976. Flake alignment in particleboard as affected by machine variables and particle geometry. Research Paper 275. USDA, Forest Products Lab., Madison, WI.

HARRIS, R. A. AND J. A. JOHNSON. 1982. Characterization of flake orientation in flakeboard by the von Mises probability distribution function. Wood Fiber 14(4): 254-266.

LANG, E. M. AND M. P. WOLCOTT. 1996. A model for viscoelastic consolidation of wood strand mats. Part I. Structural characterization of the mat via Monte Carlo simulation. Wood Fiber Sci. 28(1):100-109.

LAU, P. W. C. 1981. Numerical approach to predict the modulus of elasticity of oriented waferboard. Wood Sci. Technol. 14:73-85.

LU, C., P. R. STEINER, AND F. LAM. 1998. Simulation study of wood-flake composite mat structures. Forest Prod. J. 48(5):89-93.

MARDIA, K. V. 1972. Statistics of directional data. Academic Press, London, U.K.

PFLEIDERER, S., D. G. A. BALL, AND R. C. BAILEY. 1993. AUTO: A computer determination of the two-dimensional autocorrelation function of digital images. Computers and Geosciences 19(6):825-829.

SHALER, S. M. 1991. Comparing two measures of flake alignment. Wood Sci. Technol. 26:53-61.

SUCHSLAND, O., AND H. XU. 1989. A simulation of the horizontal density distribution in a flakeboard. Forest Prod. J. 39(5):29-33.

TRICHE, M. H., AND M. O. HUNT. 1993. Modeling of parallel-aligned wood strand composites. Forest Prod. J. 43(11/12):33-44.

VANMARCKE, E. 1983. Random fields: Analysis and synthesis. The MIT Press, Cambridge, MA, London, U.K.

XU, W., AND P. R. STEINER. 1995. A statistical characterization of the horizontal density distribution in flakeboard. Wood Fiber Sci. 27(2):160-167.

APPENDIX A

Since the concentration factor  $k = 0$  in completely randomized case, the Eq. (10) can be simplified to:

$$\alpha(\lambda, \omega, \theta_1, k, r) = \frac{1}{\theta_1} \int_{\Omega} \left(1 - \frac{r}{\omega} \sin \theta\right) \left(1 - \frac{r}{\lambda} \cos \theta\right) d\theta \quad (A.1)$$

where  $\Omega$  and  $\theta_1$  are the integration values specified as follows:

Case 1:  $\arcsin(\omega/\lambda) < \theta_1 \leq \pi/2$

$$\Omega = \begin{cases} 0 < \theta \leq \theta_1 & \left(0 < r \leq \frac{\omega}{\sin \theta_1}\right) \\ 0 < \theta \leq \arcsin\left(\frac{\omega}{r}\right) & \left(\frac{\omega}{\sin \theta_1} < r \leq \lambda\right) \\ \arccos\left(\frac{\lambda}{r}\right) < \theta \leq \arcsin\left(\frac{\omega}{r}\right) & \left(\lambda < r \leq \sqrt{\lambda^2 + \omega^2}\right) \end{cases} \quad (A.2)$$

Case 2:  $\arcsin(\omega/\sqrt{\lambda^2 + \omega^2}) < \theta_1 \leq \arcsin(\omega/\lambda)$

$$\Omega = \begin{cases} 0 < \theta \leq \theta_1 & (0 < r \leq \lambda) \\ \arccos\left(\frac{\lambda}{r}\right) < \theta \leq \theta_1 & \left(\lambda < r \leq \frac{\omega}{\sin \theta_1}\right) \\ \arccos\left(\frac{\lambda}{r}\right) < \theta \leq \arcsin\left(\frac{\omega}{r}\right) & \left(\frac{\omega}{\sin \theta_1} < r \leq \sqrt{\lambda^2 + \omega^2}\right) \end{cases} \quad (A.3)$$

Case 3:  $0 < \theta_1 \leq \arcsin(\omega/\sqrt{\lambda^2 + \omega^2})$

$$\Omega = \begin{cases} 0 < \theta \leq \theta_1 & (0 < r \leq \lambda) \\ \arccos\left(\frac{\lambda}{r}\right) < \theta \leq \arcsin\left(\frac{\omega}{r}\right) & \left(\lambda < r \leq \frac{\lambda}{\cos \theta_1}\right) \end{cases} \quad (A.4)$$

Apply Eqs. (A.2), (A.3) and (A.4) to Eq. (A.1), the Eqs. (12), (13) and (14) are obtained.

APPENDIX B

Substituting Eq. (15) into Eq. (19), the characteristic area for completely randomized strand orientation is expressed as:

$$A\left(\lambda, \omega, \frac{\pi}{2}, 0\right) = \int_0^{\sqrt{\lambda^2 + \omega^2}} 2\pi r \cdot \alpha\left(\lambda, \omega, \frac{\pi}{2}, 0, r\right) dr$$

$$= \int_0^\omega \left\{ 2\pi r - 4r \cdot \left[ \frac{r}{\lambda} + \frac{r}{\omega} - \frac{r^2}{2\lambda\omega} \right] \right\} dr \tag{B.1}$$

$$= \int_\omega^\lambda 4r \cdot \left[ \arcsin\left(\frac{\omega}{r}\right) - \frac{\omega}{2\lambda} - \frac{r}{\omega} + \frac{\sqrt{r^2 - \omega^2}}{\omega} \right] dr \tag{B.2}$$

$$+ \int_\lambda^{\sqrt{\lambda^2 + \omega^2}} 4r \cdot \left[ \arcsin\left(\frac{\omega}{r}\right) - \arccos\left(\frac{\lambda}{r}\right) - \frac{\lambda^2 + \omega^2 + r^2}{2\lambda\omega} + \frac{\sqrt{r^2 - \omega^2}}{\omega} + \frac{\sqrt{r^2 - \lambda^2}}{\lambda} \right] dr \tag{B.3}$$


---

Expressions B.1, B.2 and B.3 can be evaluated to:

$$B.1 = -\frac{5}{6} \frac{\omega^3}{\lambda} + \omega^2\pi - \frac{4}{3}\omega^2 \tag{B.4}$$

$$B.2 = 2\lambda^2 \arcsin \frac{\omega}{\lambda} + \frac{4}{3} \frac{(\lambda^2 - \omega^2)^{3/2}}{\omega} - \frac{4}{3} \frac{\lambda^3}{\omega} \tag{B.6}$$

$$+ 2\omega\sqrt{\lambda^2 - \omega^2} - \lambda\omega - \omega^2\pi + \frac{4}{3}\omega^2 + \frac{\omega^3}{\lambda} \tag{B.5}$$

$$B.3 = 2(\lambda^2 + \omega^2) \left( \arcsin \frac{\omega}{\sqrt{\lambda^2 + \omega^2}} + \arcsin \frac{\lambda}{\sqrt{\lambda^2 + \omega^2}} \right) \tag{B.7}$$

$$- \pi(\lambda^2 + \omega^2) + 2\lambda\omega - 2\lambda^2 \arcsin \frac{\omega}{\lambda}$$

$$- 2\omega\sqrt{\lambda^2 - \omega^2} - \frac{4}{3} \frac{(\lambda^2 - \omega^2)^{3/2}}{\omega} - \frac{1}{6} \frac{\omega^3}{\lambda} + \frac{4}{3} \frac{\lambda^3}{\omega}$$

Therefore, Eq. (19) is obtained by adding expressions B.4, B.5, and B.6 together and making use of the factor:

$$\arcsin \frac{\lambda}{\sqrt{\omega^2 + \lambda^2}} + \arcsin \frac{\omega}{\sqrt{\omega^2 + \lambda^2}} = \frac{\pi}{2} \tag{B.7}$$